Cancer Gene Therapy (2014) 21, 115–125

www.nature.com/cgt

ORIGINAL ARTICLE

Antitumor activity and immunogenicity of recombinant vaccinia virus expressing HPV 16 E7 protein SigE7LAMP is enhanced by high-level coexpression of IGFBP-3

J Musil, L Kutinova, K Zurkova, P Hainz, K Babiarova, J Krystofova and S Nemeckova

We constructed recombinant vaccinia viruses (VACVs) coexpressing the *insulin-like growth factor-binding protein-3* (*IGFBP-3*) gene and the fusion gene encoding the SigE7Lamp antigen. The expression of the IGFBP-3 transgene was regulated either by the early H5 promoter or by the synthetic early/late (E/L) promoter. We have shown that IGFBP-3 expression regulated by the H5 promoter yielded higher amount of IGFBP-3 protein when compared with the E/L promoter. The immunization with P13-SigE7Lamp-H5-IGFBP-3 virus was more effective in inhibiting the growth of TC-1 tumors in mice and elicited higher T-cell response against VACV-encoded antigen than the P13-SigE7Lamp-TK$^-$ control virus. We found that high-level production of IGFBP-3 enhanced virus replication both *in vitro* and *in vivo*, resulting in more profound antigen stimulation. Production of IGFBP-3 was associated with a higher adsorption rate of P13-SigE7Lamp-H5-IGFBP-3 to CV-1 cells when compared with P13-SigE7Lamp-TK$^-$. Intracellular mature virions (IMVs) of the IGFBP-3-expressing virus P13-SigE7Lamp-H5-IGFBP-3 have two structural differences: they incorporate the IGFBP-3 protein and they have elevated phosphatidylserine (PS) exposure on outer membrane that could result in increased uptake of IMVs by macropinocytosis. The IMV PS content was measured by flow cytometry using microbeads covered with immobilized purified VACV virions.

Cancer Gene Therapy (2014) **21,** 115–125; doi:10.1038/cgt.2014.6; published online 21 February 2014

Keywords: IGFBP-3; vaccinia virus; HPV16 E7; T-cell response; tumor; phosphatidylserine

INTRODUCTION

The vaccinia virus (VACV) has been studied as a recombinant vector for the treatment of cancer. Various recombinant VACVs expressing tumor-associated antigens were constructed. During the 1980s, several methods for the insertion of foreign DNA into the VACV genome and subsequent selection of recombinant viruses have been developed.[1] Subsequently, synthetic promoters have been created to enhance the expression of the inserted transgenes.[2] These methods allowed the construction of recombinant VACV (rVACV) expressing different tumor-associated antigens, that is, CEA, PSA, MUC-1, 5T4, Melan-A and others.[3–7] It has been shown that rVACV can induce antibodies and T cell-mediated responses against the expressed tumor-associated antigen. To further enhance the immunogenicity of the tumor-associated antigen-expressing rVACV, the genes encoding costimulatory molecules such as B7-1, ICAM-1 and LFA-3 and cytokines such as IL-2, GM-CSF, Flt3L and so on have been inserted in poxvirus vectors.[8–11] Several of these approaches have also been tested in clinical trials.[12–15] The tested viruses have been shown to be well tolerated and immunogenic, but thus far clinical responses have been rather disappointing. The failure to elicit clinical responses can be attributed to the immunodominance of the vaccinia vector or may be caused by tumor immune evasion strategies.[16–18]

Two forms of infectious virions can be detected in infected cells: intracellular mature virus (IMV) and extracellular enveloped virus. Mercer and Helenius[19] have shown that IMV employs macropinocytosis and apoptotic mimicry to enter host cells. The outer membrane of IMV is enriched in phosphatidylserine (PS), and thus virions resembling apoptotic bodies are internalized by macropinocytic response of many types of cells.

Insulin-like growth factor-binding protein-3 (IGFBP-3), first identified as a major carrier protein prolonging the half-life of insulin-like growth factor-I (IGF-I) in the bloodstream, has been recognized as an important regulator of growth, regeneration, senescence and tumorigenesis.[20–24] In the context of cancer, IGFBP-3 has been intensively studied for its growth inhibitory properties and as a protein involved in the induction of apoptosis. IGFBP-3 exerts its inhibitory effects by IGF-dependent and IGF-independent mechanisms. It has been shown that IGFBP-3 binds IGF with greater affinity than the IGF receptor (IGF-R), which enables it to sequester IGF interacting with IGF-R.[25] The sequestration of IGF by IGFBP-3 is coupled with downregulation of IGF-R-stimulated prosurvival mitogen-activated protein kinase and Akt pathways.[26,27]

Experiments using either IGFBP-3 mutants lacking IGF-binding activity, IGFBP-3-derived fragments or IGF-R-negative cells have shown evidence for IGF-independent inhibitory effects of IGFBP-3.[28] The IGF-independent effects of IGFBP-3 are based on several different mechanisms. These include binding to receptors on the cell surface and receptor-mediated growth inhibition or induction of apoptosis via caspase-8 activation.[28,29]

The activation of caspase-8 by IGFBP-3 and subsequent activation of caspases-3/7 causes not only the induction of apoptosis, but also leads to degradation of p65-nuclear factor-κB that results in downregulation of nuclear factor-κB-regulated factors involved in angiogenesis such as vascular endothelial growth factor and interleukin-8.[30,31]

Department of Experimental Virology, Institute of Hematology and Blood Transfusion, Prague, Czech Republic. Correspondence: Dr S Nemeckova, Department of Experimental Virology, Institute of Hematology and Blood Transfusion, U Nemocnice 1, Prague 2 128 20, Czech Republic.
E-mail: nemeckova@uhkt.cz
Received 1 October 2013; revised 31 January 2014; accepted 31 January 2014; published online 21 February 2014

Extracellular IGFBP-3 can be internalized by several endocytic pathways that include caveolar, clathrin-mediated and, to a lesser extent, fluid-phase endocytosis.[32] Clathrine-mediated endocytosis of IGFBP-3 is mediated via interactions with transferrin and the transferrin receptor, whereas the caveolar endocytotic pathway includes binding of IGFBP-3 to caveolin-1.[33,34] IGFBP-3 is then shuttled through the endosome/lysosome compartment to the nucleus. The nuclear import is then mediated by interactions with importin-β.[35] In the nucleus, IGFBP-3 interacts with a number of binding partners that results in the induction of apoptosis[36] and cell cycle arrest in the G-1 phase.[37,38] Cancer cells can acquire resistance to IGFBP-3-mediated growth inhibition, for example, by the expression of constitutively active Ras.[39]

Cancer cells often downregulate IGFBP-3 expression by increasing the methylation of the IGFBP-3 promoter and positive transcription regulatory elements.[40–43] The expression of IGFBP-3 can also be decreased because of the loss of inducing transcription factors.[44,45] The amount of intracellular IGFBP-3 is determined by protein stability. The ubiquitination and subsequent degradation in the proteasome have been shown to regulate the amount of IGFBP-3 in the nucleus.[46] In cervical cancer, the papillomavirus E7 oncoprotein inhibits the function of IGFBP-3 in the nucleus by increasing its degradation in the ubiquitin–proteasome proteolytic pathway.[47]

In the present study we wanted to investigate whether the tumor-suppressive properties of IGFBP-3 can enhance the efficacy of therapeutic immunization against the HPV16 E7 oncogene that is associated with cervical cancer. For this reason, we created double recombinant VACVs expressing IGFBP-3 and the fusion gene SigE7Lamp. The analysis of the tumor inhibitory effect induced by the P13-SigE7Lamp-H5-IGFBP-3 recombinant virus has found association between high-level expression of IGFBP-3 and virus replication. Further investigation has shown that IGFBP-3 is integrated into the IMV virion and that the virion outer membrane has increased content of PS, and this is what probably contributes to the increased adsorption rate of this virus.

MATERIALS AND METHODS

Plasmids

The coding sequence of human IGFBP-3 was obtained in the pXBP-3WT plasmid.[46] The restriction site for *Xho*I in pXBP-3WT was deleted by cleavage with *Xho*I and *Sal*I and subsequent ligation. The resulting plasmid was denoted pXBP3-WTΔXhoI. The IGFBP-3 sequence was excised from pXBP3-WTΔXhoI by *Xba*I and inserted in the pUC131 plasmid cut by the same enzyme creating pUC131-IGFBP-3. Finally, the IGFBP-3 coding sequence was excised with the *Xho*I and *Eco*RI restriction enzymes from pUC131-IGFBP-3 and inserted into pSC59-H5[48] cut by the same restriction endonucleases. The resulting plasmid was denoted pSC59-E/L-IGFBP-3. The recombination plasmid pSC59-H5-IGFBP-3 was created by the excision of the early/late (E/L) promoter from pSC59-E/L-IGFBP-3 with *Sal*I restriction endonuclease and ligation.

Viruses and cells

The clone 13 of vaccinia virus strain Praha, previously prepared and characterized in our laboratory,[49] was used as the parental virus. The coding sequence of IGFBP-3 was inserted into the thymidine kinase gene of vaccinia virus P13 or P13-SigE7LAMP behind the early H5 or synthetic E/L promoter. The virus P13-SigE7LAMP[50] used for recombination carries SigE7LAMP fusion gene inserted in the F7L locus. Recombinant viruses were prepared by the method described by Perkus *et al.*[51] The plasmids pSC59-H5-IGFBP-3 and pSC59-E/L-IGFBP-3 were used for the generation of recombinant viruses denoted P13-H5-IGFBP-3, P13-E/L-IGFBP-3, P13-SigE7Lamp-H5-IGFBP-3 and P13-SigE7Lamp-E/L-IGFBP-3. The control virus P13-SigE7Lamp-TK$^-$ has the TK gene disrupted by the insertion of 100 bp derived from the VACV 11k promoter. The virus P13-preS2S with expression of hepatitis B virus envelope antigen has been described previously.[52] Viruses were propagated in BSC40 cells in Dulbecco's modified Eagle's medium (PAA, Pasching, Austria) supplemented with 10% fetal bovine serum (PAA). Virus (IMV) was purified by sucrose gradient centrifugation.[53] Briefly, cells were harvested at 48 h after infection, pelleted by centrifugation (53 000 *g*, 4 °C, 60 min), resuspended in serum-free Dulbecco's modified Eagle's medium and pelleted (53 000 *g*, 4 °C, 40 min). The pellet was resuspended in 3 ml of extraction buffer (1 mM $Na(PO_4)$, pH 9) and disrupted by sonication (3 × 5 min on ice). The cell debris was pelleted at 4500 *g* at 4 °C for 10 min, resuspended in 3 ml of fresh extraction buffer, sonicated and cell debris was pelleted as above. Both supernatant fractions were layered on 10 ml 36% sucrose in 1 mM Tris, pH 8, and centrifuged at 29 800 *g* at 4 °C for 90 min. The pellet was resuspended in 1 ml of extraction buffer, sonicated, layered on 30 ml of sucrose gradient (20–45%) and centrifuged as above. The opalescent zone was diluted to 30 ml with extraction buffer and pelleted 53 000 *g* at 4 °C for 60 min. The pellet containing mainly IMV was resuspended and the virus was titrated in CV-1 cells. HPV16 E6E7-expressing TC-1 cells[54] and HPV16 E6E7-expressing major histocompatibility complex class I-negative MK16/1/IIIABC (abbreviated as MK16/ABC)[55] were both derived from C57BL/6 mouse. CV-1, MK16/ABC and TC-1 cells were cultured in Eagle's minimum essential medium (Sigma-Aldrich, St Louis, MO, USA) supplemented with 5% fetal bovine serum (PAA) and minimum essential medium vitamins (PAA).

Enzyme-linked immunosorbent assay (ELISA) IGFBP-3

IGFBP-3 was quantified using the DuoSet Elisa Development System–human IGFBP-3 (R&D Systems, Minneapolis, MN, USA). The absorbance was measured by an ELISA reader at 450 nm.

Detection of VACV multiplication *in vivo* using quantitative PCR

Virus DNA in infected mice was detected as described previously.[11]

Assay of T-cell immune response

Mice were intraperitoneally immunized with recombinant VACV. They were killed 12 days after immunization, their spleens were removed and lymphocytes were isolated. The response of interferon-γ-producing cells was determined by enzyme-linked immunosorbent spot (ELISPOT) in the *ex vivo* setting, as described previously.[50] Lymphocytes were stimulated with H-2Db-restricted HPV16 E7(49–57) (RAHYNIVTF) or VACV E3(140–148) (VGPSNSPTF) peptide for 20 h.[56]

Animal experiments

Six-week-old female C57BL/6(H-2b) mice were obtained from Charles River, Sulzfeld, Germany. The animals were maintained under standard conditions at the National Institute of Public Health (Prague, Czech Republic). All experiments were performed in compliance with Acts No. 246/92 and 77/2004 on animal protection against cruelty, and Decree No. 311/97 of the Ministry of Health of the Czech Republic, on the care and use of experimental animals.

Tumor induction

Mice received a dose of 3×10^5 MK16/ABC or 6×10^4 TC-1 tumor cells injected subcutaneously in 0.1 ml RPMI-1640 into the back. Tumor growth was measured weekly.

Sodium dodecyl sulfate-polyacrylamide gel electrophoresis (SDS-PAGE) and western blot

Purified virus particles were mixed with sample buffer (100 mM Tris-Cl, pH = 6.8; 2% SDS; 20% glycerol; and 4% β-mercapthoethanol) and separated by SDS-PAGE on 10% gels. The separated proteins were blotted onto a nitrocellulose membrane (Hybond-C extra, Amersham plc, Amersham, UK). After blocking with 10% nonfat dry milk in phosphate-buffered saline (PBS), the membrane was incubated with goat biotinylated primary antibody BAF675 (anti-hIGFBP-3, R&D Systems) diluted 1:200. After washing, the membrane was incubated with horseradish peroxidase-conjugated avidin (BD Pharmingen, San Diego, CA, USA). Proteins were visualized with the enhanced chemiluminiscence system (ECL Plus system, Amersham).

Fractionation of VACV virions

Samples of virions purified by sucrose gradient centrifugation containing equal amounts of proteins as determined by the Bio-RAD protein assay (Bio-Rad, Hercules, CA, USA) were subsequently incubated in 50 mM Tris buffer with 10 mM $MgCl_2$, pH 8.5, supplemented with 1% NP-40 at 37 °C for 30 min to solubilize the membrane fraction (M); 1% NP-40 plus 50 mM

dithiothreitol for matrix-like fraction (MX); and 0.5% deoxycholate and 0.1% SDS for the soluble core fraction (C1). Each fraction was separated from insoluble sediment (C2) after centrifugation at 13 000 *g* for 15 min.[57,58]

VACV neutralization

Petri dishes with a 24-h culture of CV-1 cells were infected with 200 μl of virus suspension to yield ~150 plaques per dish. After 1.5 h of adsorption at 37 °C, 200 μl of VACV-neutralizing rabbit serum or control rabbit serum diluted 1:5 in the medium, or the medium alone was added for 1 h at 37 °C. The inoculum was removed and cells were overlaid with 1% agar supplemented with Eagle's minimum essential medium and 5% fetal bovine serum. After 3 days at 37 °C, 1% agar supplemented with the medium and neutral red was overlaid and plaques were counted.

Adsorption assay

CV-1 cell cultures were inoculated as in the neutralization assay. At indicated intervals, the inoculum was removed and stored at −70 °C. Virus concentration in the inoculum was determined by the plaque assay.

Statistical analysis

Statistical analyses were calculated using the Prism 5.0 software (GraphPad Software, San Diego, CA, USA).

PS detection on virions

One drop containing 100 000 beads of size 7–9 μm with covalently linked protein G (Flow Cytometry Protein G Antibody Binding Beads purchased from Bangs Laboratories, Fishers, IN, USA) was placed into a test tube together with 20 μl of anti-VACV mouse serum (1:1 in PBS). The serum from naive mouse was used as control. After 30 min of incubation, 100 μl blocking buffer (1%BSA, 10% fetal bovine serum, 0.1% NaN_3 in PBS) was added and incubated for additional 30 min under occasional rocking. The beads were washed twice with PBS (always centrifugation 300 *g* per 2 min). The presence of mouse IgG on beads was confirmed in one aliquot by staining with the anti-mouse Fab IgG AlexaFluor488 conjugate (Molecular Probes, Eugene, OR, USA). The beads were measured by flow cytometry (Supplementary Figure 1). In the next step, purified virions (48 μg protein) in 20 μl were mixed with anti-VACV IgG-coated beads and incubated under occasional rocking for 3 h. The beads were washed twice as above and resuspended in 20 μl of the blocking buffer. To examine whether the beads have been covered with virions, an aliquot was mixed with 20 μl of rabbit anti-VACV serum. After 30 min of incubation, the beads were twice washed with blocking buffer and stained with 5 μl donkey anti-rabbit IgG-DyLight 649 (Biolegend, San Diego, CA, USA) and analyzed by flow cytometry (Supplementary Figure 2). Beads covered with virions were used for further analysis. The beads were mixed with 200 μl of blocking buffer and incubated for 5 min and washed twice with PBS. Finally, the beads were transferred to 50 μl annexin binding buffer and stained with 5 μl phycoerythrin-labeled annexin V (BD Biosciences, San Jose, CA, USA) for 15 min at room temperature. In the next step, the beads were centrifuged and resuspended in fresh annexin binding buffer and analyzed by flow cytometry. All flow cytometry measurements were performed with LSRFortessa 5L flow cytometer (BD Biosciences) and analyzed by FlowJo 7.6.5 software (TreeStar, Ashland, OR, USA). All incubations were performed on ice.

RESULTS

High-level expression of IGFBP-3 driven by the early H5 promoter

First, we determined the production of IGFBP-3 protein by rVACV. CV-1 cells were infected at the multiplicity of infection of 0.1 with P13-SigE7Lamp-TK$^-$, P13-SigE7Lamp-H5-IGFBP-3 or P13-SigE7Lamp-E/L-IGFBP-3. Infected cell cultures were frozen at −70 °C and thawed. The cells in the medium were sonicated three times for 1 min. The cell debris was removed by centrifugation for 20 min at 830 *g*. Concentration of hIGFBP-3 was measured by ELISA. To exclude the influence of casual mutations, the independently prepared sister viruses, denoted P13-SigE7Lamp-H5-IGFBP-3(b) and P13-SigE7Lamp-E/L-IGFBP-3(b), were also included in the experiment. We observed that the production of IGFBP-3 at 48 and 72 h after infection was significantly higher (***$P<0.001$) when the H5 promoter was used rather than the E/L promoter (Figure 1). The difference in IGFBP-3 production was stable in the three repeated experiments.

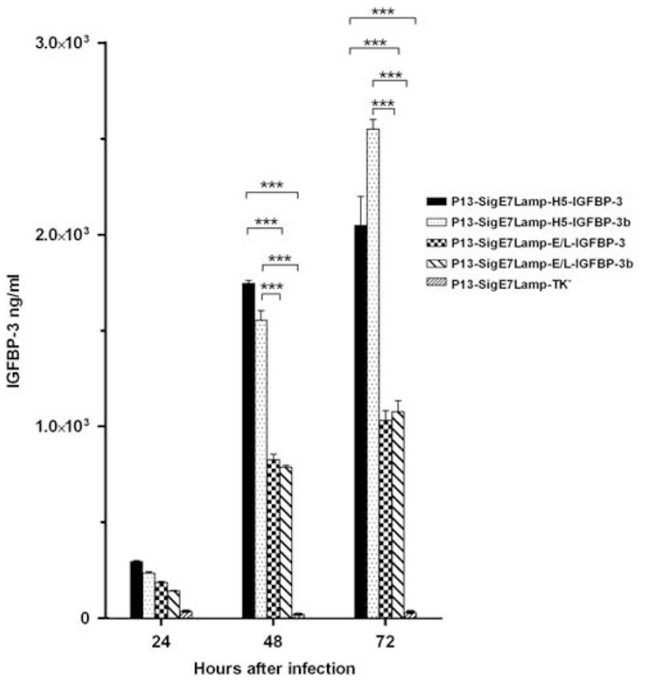

Figure 1. The H5 promoter drives higher expression of insulin-like growth factor-binding protein-3 (IGFBP-3) than the early/late (E/L) promoter. CV-1 cells were infected at a multiplicity of infection (MOI) of 0.1 with P13-SigE7Lamp-H5-IGFBP-3, P13-SigE7Lamp-E/L-IGFBP-3 and independently prepared sister viruses P13-SigE7Lamp-H5-IGFBP-3(b) and P13-SigE7Lamp-E/L-IGFBP-3(b). After 2 h of adsorption at 37 °C, the cells were washed three times and fresh medium was added. At indicated intervals, the cultures were frozen and thawed, sonicated three times for 1 min and the cell debris was removed by centrifugation at 830 *g*. IGFBP-3 concentration was determined by enzyme-linked immunosorbent assay (ELISA) in duplicate. Statistical significance was calculated using two-way analysis of variance (ANOVA). ***$P<0.001$.

Coexpression of IGFBP-3 enhances VACV-specific T-cell responses

In the next step, we investigated whether IGFBP-3 expression by our rVACV could enhance the induction of T-cell immune responses. Mice ($n=4$) were intraperitoneally immunized with one dose of 3×10^6 PFUs of P13-SigE7Lamp-TK$^-$, P13-SigE7Lamp-H5-IGFBP-3 or P13-SigE7Lamp-E/L-IGFBP-3 viruses. The T-cell response against HPV 16 E7 peptide or VACV E3 peptide was determined by enzyme-linked immunosorbent spot (ELISPOT) interferon-γ. As can be seen in Figure 2, the differences in the immune response against E7 oncogene between mice immunized with P13-SigE7Lamp-TK$^-$, P13-SigE7Lamp-H5-IGFBP-3 or P13-SigE7Lamp-E/L-IGFBP-3 were detected. All three recombinant viruses induced cytotoxic T lymphocyte responses against the HPV16 E7 nonapeptide.[49–57] Coexpression of IGFBP-3 enhanced the E7-specific response only subtly. The enhancement of the T-cell response by IGFBP-3 coexpression was more apparent against the VACV E3-derived peptide in mice receiving P13-SigE7Lamp-H5-IGFBP-3 and P13-SigE7Lamp-E/L-IGFBP-3. However, the difference was not statistically significant because of high variability.

High-level expression of IGFBP-3 in combination with E7-specific immunization inhibits tumor growth

The next step was to determine the effect of IGFBP-3 expressed by VACV on the preventive and therapeutic vaccination against

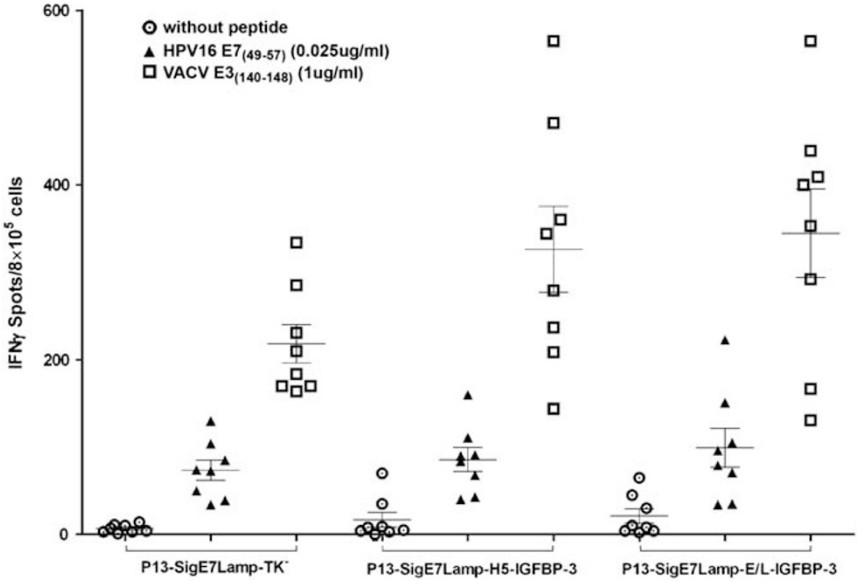

Figure 2. Enhancement of vaccinia virus (VACV)-specific T-cell responses by coexpression of insulin-like growth factor-binding protein-3 (IGFBP-3). Groups of mice ($n = 4$) were immunized with 3×10^6 plaque-forming units (PFUs) per 0.5 ml phosphate-buffered saline (PBS) of P13-SigE7Lamp-TK$^-$, P13-SigE7Lamp-H5-IGFBP-3 or P13-SIgE7Lamp-E/L-IGFBP-3. After 12 days, their spleens were removed and response of interferon-γ (IFN-γ)-producing cells was determined by enzyme-linked immunosorbent spot (ELISPOT) IFN-γ in two parallels. Each symbol represents one well in ELISPOT plate. The mean of each group is indicated by horizontal line, s.d. by the error bars.

E7 antigen. Female C57BL/6(H-2b) mice were intraperitoneally immunized with 1×10^6 PFUs of rVACV either 2 weeks before subcutaneous injection of 3×10^5 MK16/ABC cells or 10 days after injection of 6×10^4 TC-1 cells. Preventive vaccination with P13-SigE7Lamp-H5-IGFBP-3 significantly inhibited the growth of MK16/ABC tumors. The mean size of tumors was smaller by days 39, 46 and 53 after challenge (Figure 3a) when compared with treatment with P13—H5-IGFBP-3 or P13-preS2S virus. In the therapeutic arrangement, mice have carried palpable TC-1 tumors at the time of treatment. Administration of P13-SigE7Lamp-H5-IGFBP-3 significantly inhibited the growth of TC-1 tumors ($^*P < 0.05$) by day 11 after virus injection (Figure 3b) when compared with PBS treatment, whereas mice treated with P13-SigE7Lamp-TK$^-$ or P13-SigE7Lamp-E/L-IGFBP-3 had not significantly smaller tumors until day 18 ($^{***}P < 0.001$). Moreover, the treatment with P13-SigE7-Lamp-H5-IGFBP-3 resulted in significantly smaller tumors on day 32 ($^*P < 0.05$) when compared with P13-SigE7Lamp-TK$^-$. These results were repeatedly confirmed (data not shown). Treatment with P13-E/L-IGFBP-3 or P13-preS2S control virus was without a significant therapeutic effect (Figure 3c) that indicates that IGFBP-3 alone is unable to slow down tumor growth.

High-level expression of IGFBP-3 enhances virus replication

To explain the increased immunogenicity and enhanced therapeutic effect of P13-SigE7Lamp- H5-IGFBP-3, we decided to test whether IGFBP-3-expressing viruses could replicate better than the virus P13-SigE7Lamp-TK$^-$. At first, we determined the viral replication *in vivo*. The C57BL/6(H-2b) mice were infected with 1×10^6 PFUs of rVACV and viral DNA was measured by quantitative PCR in their ovaries at the indicated times (Figure 4). The results showed a higher replication rate of P13-SigE7Lamp-H5-IGFBP-3 on day 3 when compared with P13-SigE7Lamp-TK$^-$ and P13-SigE7Lamp-E/L-IGFBP-3 (Figure 4). On day 4, higher levels of viral DNA were observed in mice infected with P13-SigE7Lamp-H5-IGFBP-3 and P13-SigE7Lamp-E/L-IGFBP-3, but the differences were not significant because of high variance in the *in vivo* experiment.

To confirm that the behavior of rVACV observed *in vivo* also occurs *in vitro*, in the next step, we compared viral replication in cultures of CV-1 cells and murine TC-1 cells. The cells grown for 24 h to full confluence were infected with P13-SigE7Lamp-TK$^-$, P13-SigE7Lamp- H5-IGFBP-3 or P13-SigE7Lamp-E/L-IGFBP-3 at the multiplicity of infection of 0.1. After 48 h, the culture media and cells were harvested and sonicated and the cell debris was removed by centrifugation. The amount of IGFBP-3 was measured by ELISA and virus content was determined by titration on CV-1 cells. The results showed that the replication of P13-SigE7Lamp-H5-IGFBP-3 was significantly higher when compared with P13-SigE7Lamp-TK$^-$ in both CV-1 and TC-1 (Table 1). The viruses P13-SigE7Lamp-E/L-IGFBP-3 and P13-SigE7Lamp-TK$^-$ do not seem to differ in their ability to replicate in TC-1 cells, but when CV-1 cells are used, the virus P13-SigE7Lamp-E/L-IGFBP-3 replicates significantly better than the virus P13-SigE7Lamp-TK$^-$. When the cells were infected at a multiplicity of infection of 2.0, similar differences in virus replication were found after 24 h (data not shown). Higher growth rate of recombinant viruses was confirmed by the same results with the independently prepared sister virus P13-SigE7Lamp-TK$^-$(b) that was used in another experiment (data not shown).

We therefore assumed that the amount of produced IGFBP-3 played a key role in the enhancement of virus replication. To test this hypothesis, we repeated the virus growth experiment in the presence of the neutralizing goat polyclonal antibody AF675 (anti-human IGFBP-3, R&D Systems). After a 2-h virus adsorption, cells were washed and fresh medium containing $4\,\mu g\,ml^{-1}$ of anti-IGFBP-3 antibody or PBS was added. After 24 h of culture at 37 °C, another aliquot of anti-IGFBP-3 antibody was added. At 48 h after infection, the cells and media were harvested and the amounts of IGFBP-3 and virus were determined. It was found that the presence of the anti-IGFBP-3 antibody significantly ($^{**}P < 0.01$) decreased both the yields of P13-SigE7Lamp-H5-IGFBP-3 (Figure 5a) and the amount of detectable IGFBP-3 (Figure 5b). Although we added $4\,\mu g\,ml^{-1}$ of anti-IGFBP-3 antibody, it was insufficient to neutralize the high amount of IGFBP-3 produced by the P13-SigE7Lamp-H5-IGFBP-3 virus.

Complete neutralization of IGFBP-3 was achieved only with P13-SigE7Lamp-TK$^-$-infected cells. In this case, adding the anti-IGFBP-3 antibody is associated with a significant ($^*P < 0.05$) increase in virus yields. The experiment was repeated twice with similar

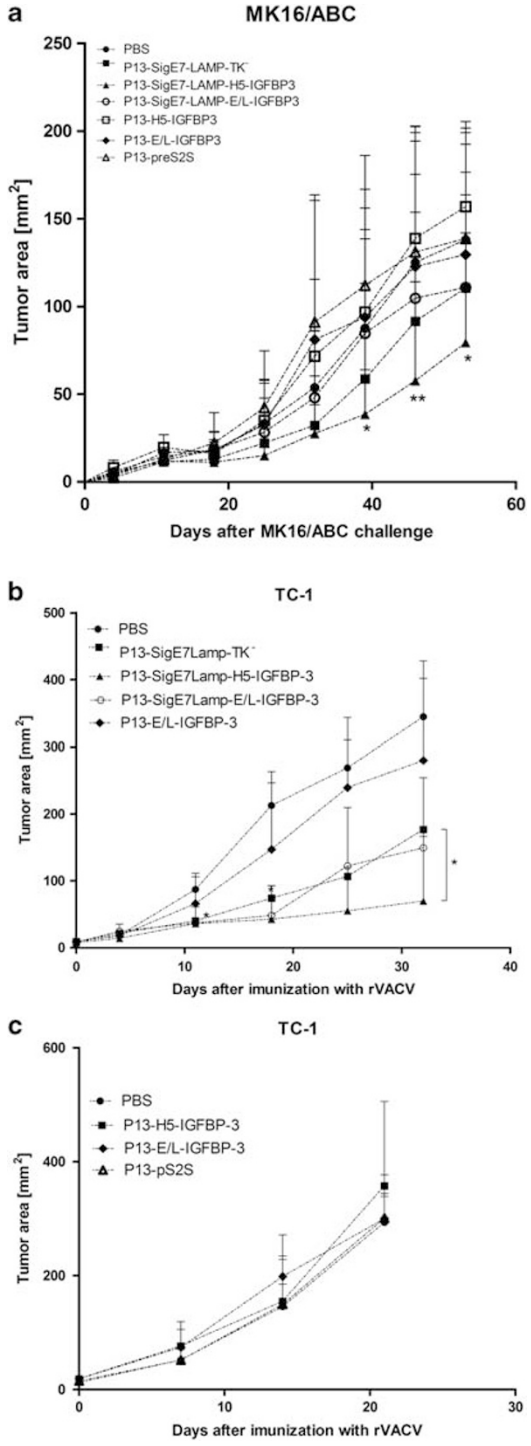

Figure 3. Tumor growth is inhibited by immunization or treatment with the P13-SigE7Lamp-H5-IGFBP-3 virus. Groups of female C57BL/6(H-2b) mice ($n = 6$) were intraperitoneally (i.p.) immunized with 1×10^6 plaque-forming units (PFUs) of double recombinant viruses coexpressing insulin-like growth factor-binding protein-3 (IGFBP-3) and SigE7Lamp and after 2 weeks subcutaneously (s.c.) injected with 3×10^5 MK16/ABC cells (**a**). Other groups were first s.c. injected with 6×10^4 TC-1 cells and after 10 days, when tumors were palpable, mice were i.p. immunized with 1×10^6 PFUs of recombinant viruses (**b**, **c**). Results were analyzed and statistics were calculated using two-way analysis of variance (ANOVA). $^*P < 0.05$, $^{**}P < 0.01$. The experiment was repeated twice with similar results.

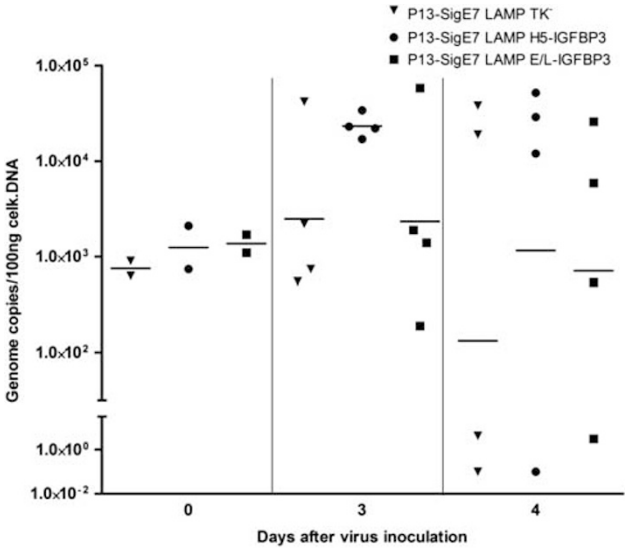

Figure 4. Expression of insulin-like growth factor-binding protein-3 (IGFBP-3) enhances virus replication *in vivo*. Groups of female C57BL/6(H-2b) mice ($n = 4$) were intraperitoneally (i.p.) infected with 1×10^6 plaque-forming units (PFUs) of recombinant vaccinia virus (rVACV). Ovaries were collected at indicated times and replication of rVACV was determined by quantitative PCR (qPCR). Geometric means are shown. Results were analyzed and statistics were calculated using two-way analysis of variance (ANOVA).

Table 1. High-level expression of IGFBP-3 enhances replication of rVACV *in vitro*

Cell line[a]	*Virus*	*Yield (PFU* $\times 10^7$*)*[b]	*IGFBP-3* (10^3 *ng ml*$^{-1}$*)*[c]
CV1	P13-SigE7Lamp-TK$^-$	2.73 ± 0.55	
CV1	P13-SigE7Lamp-H5-IGFBP-3	5.40 ± 0.67	3.74 ± 0.11
CV1	P13-SigE7Lamp-E/L-IGFBP-3	4.45 ± 0.63	1.58 ± 0.18
TC-1	P13-SigE7Lamp-TK$^-$	1.26 ± 0.11	
TC-1	P13-SigE7Lamp-H5-IGFBP-3	1.72 ± 0.20	0.73 ± 0.03
TC-1	P13-SigE7Lamp-E/L-IGFBP-3	1.08 ± 0.18	0.26 ± 0.01

Abbreviations: E/L, early/late; IGFBP-3, insulin-like growth factor-binding protein-3; PFU, plaque-forming unit; rVACV, recombinant vaccinia virus.
[a]The replication of IGFBP-3-expressing viruses was determined in CV-1 or TC-1 cells at 48 h after infection.
[b]The value represents the mean of four parallels.
[c]The IGFBP-3 concentration was measured by enzyme-linked immunosorbent assay (ELISA) in two parallels.

results. We speculate that this can be attributed to the complete neutralization of IGFBP-3 in the media. Our observation suggests that IGFBP-3 is accumulating in aging CV-1 cultures and is used to downregulate the metabolism of these cells. More metabolically active cells favor virus replication.

IGFBP-3 expressed by rVACV is incorporated into IMV

Because anti-IGFBP-3 antibody decreased the titer of the P13-SigE7Lamp-H5-IGFBP-3, we asked whether this could be because of the binding of the antibody to the IGFBP-3 integrated into IMV. We decided to detect IGFBP-3 in virions by western blot.

First, we prepared samples of purified rVACVs with equal protein content. To exclude the influence of casual mutations, we included independently prepared sister viruses

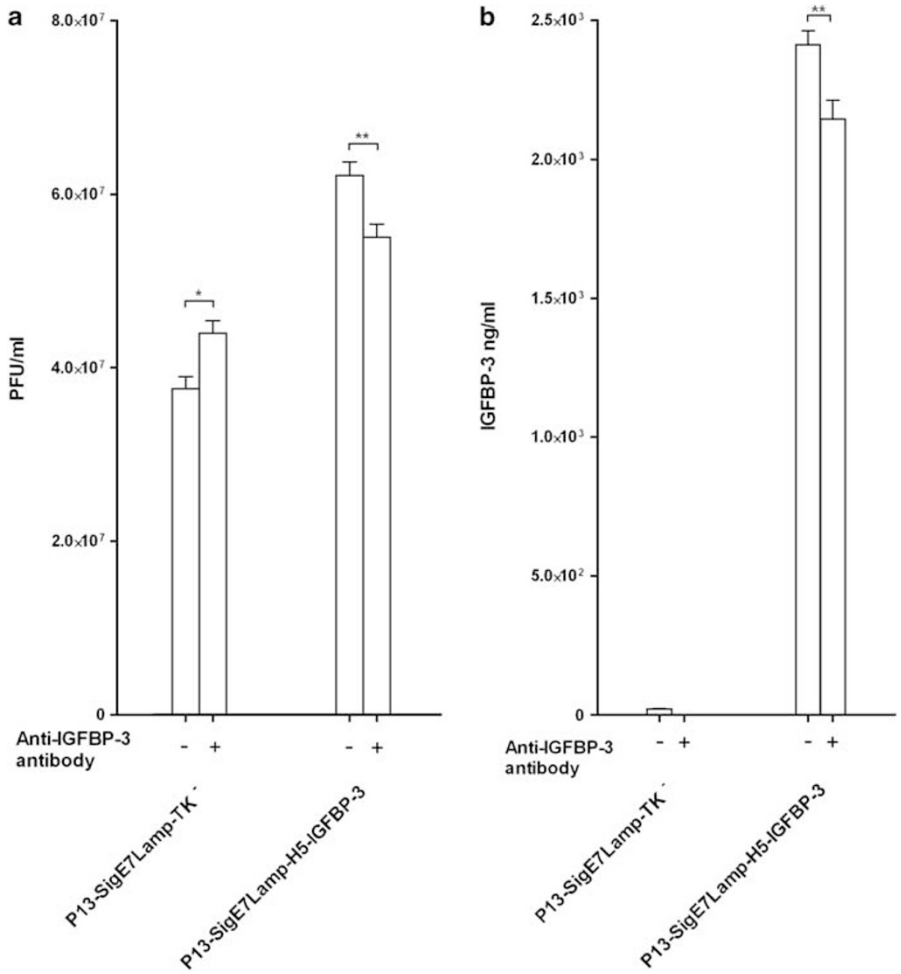

Figure 5. Neutralization of insulin-like growth factor-binding protein-3 (IGFBP-3) decreases the yield of P13-SigE7Lamp-H5-IGFBP-3. CV-1 cells were infected at a multiplicity of infection (MOI) of 0.1 with P13-SigE7Lamp-TK$^-$ or P13-SigE7Lamp-H5-IGFBP-3. After 2 h of virus adsorption, cells were washed and the medium containing either 4 μg ml^{-1} of the polyclonal goat anti-IGFBP-3 antibody or phosphate-buffered saline (PBS) was added. After 24 h of culture at 37 °C, another aliquot of anti-IGFBP3 antibody (Ab) was added. After 48 h after infection, cells were frozen at −70 °C and then thawed, sonicated and centrifuged, and the resulting supernatants were titrated in quadruplicates (**a**). The concentration of IGFBP-3 in the media was measured by enzyme-linked immunosorbent assay (ELISA) (**b**). Results were analyzed and statistics were calculated using one-way analysis of variance (ANOVA). $^{**}P < 0.01$.

P13-SigE7Lamp-TK$^-$(b), P13-SigE7Lamp- H5-IGFBP-3(b) and P13-SigE7Lamp- E/L-IGFBP-3(b). The samples were then separated on a 10% SDS-PAGE gel and blotted onto a nitrocellulose membrane. IGFBP-3 was visualized using the goat polyclonal biotin-labeled specific antibody BAF675 (anti-hIGFBP-3, R&D Systems). As can be seen in Figure 6a, we detected up to four bands (I–IV) in purified P13-SigE7Lamp-H5-IGFBP-3 and P13-SigE7Lamp-H5-IGFBP-3(b). The size of the band I corresponds to the glycosylated hIGFBP-3 standard (R&D Systems); bands II and III are of smaller size, under 25 kDa. Band IV is the largest, with a molecular weight of ~80 kDa.

We also detected bands I–III in samples prepared from IGFBP-3 in P13-SigE7Lamp-E/L-IGFBP-3 and P13-SigE7Lamp-E/L-IGFBP-3(b), but longer exposure times were required, indicating a much smaller concentration of the integrated protein.

Next, we determined the localization of IGFBP-3 to a specific compartment of the IMV. Purified P13-SigE7Lamp-TK$^-$, P13-SigE7Lamp-H5-IGFBP-3 and P13-SigE7Lamp-H5-IGFBP-3(b) particles were fractionated and the fractions were analyzed by western blot using the anti-IGFBP-3 antibody. No bands were detected in fractions of the P13-SigE7Lamp-TK$^-$ virus (Figure 6b). Only faint bands were detectable in the membrane fractions (M) of IGFBP-3-expressing viruses.

The MX of P13-SigE7Lamp-H5-IGFBP-3 or P13-SigE7Lamp-H5-IGFBP-3(b) contains IGFBP-3 (band I) and smaller bands II and III, whereas the core fraction (C1,C2) yielded IGFBP-3 band I and the larger band IV.

Finally, we determined whether the incorporation of IGFBP-3 into IMVs is associated with changes in the protein content of P13-SigE7Lamp-H5-IGFBP-3 or P13-SigE7Lamp-E/L-IGFBP-3 in comparison with P13-SigE7Lamp-TK$^-$.

Purified rVACV IMVs were separated on a 10% SDS-PAGE gel and subsequently stained with Coomassie brilliant blue. The patterns of all viruses were similar (Figure 6c), and hence we concluded that IGFBP-3 integration into IMV did not affect virion assembly.

Incorporation of IGFBP-3 into IMV affects virus adsorption

We wanted to learn which phase of the replication cycle was affected by IGFBP-3 coexpression and whether the presence of IGFBP-3 in the IMV of P13-SigE7Lamp-H5-IGFBP-3 could help the virus during the process of virus entry. The CV-1 cell monolayers were infected for 1.5 h at 37 °C with such amount of P13-SigE7Lamp-TK$^-$ and P13-SigE7Lamp-H5-IGFBP-3 to yield ~150

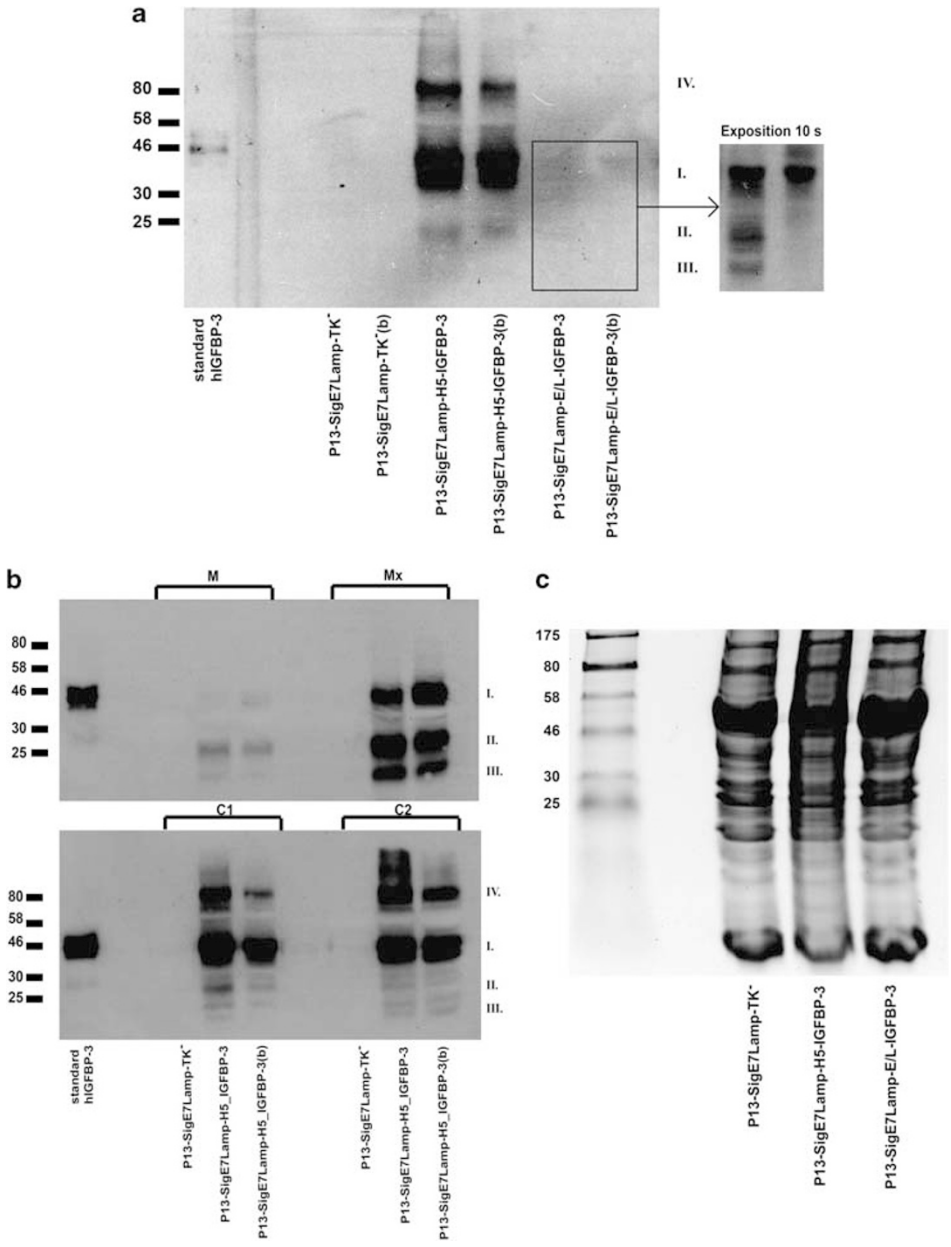

Figure 6. Insulin-like growth factor-binding protein-3 (IGFBP-3) is incorporated into recombinant vaccinia virus (rVACV) virions but does not disrupt virion structure. The amount of the protein was determined for each sucrose purified virus suspension by the Bio-RAD protein assay. Equal amounts of purified virions of P13-SigE7Lamp-TK$^-$, P13-SigE7Lamp-TK$^-$(b), P13-SigE7Lamp-H5-IGFBP-3, P13-SigE7Lamp-H5-IGFBP-3(b), P13-SigE7Lamp-E/L-IGFBP-3 and P13-SigE7Lamp-E/L-IGFBP-3(b) were dissolved in sample buffer heated to 100 °C for 5 min. The proteins were separated on 10% sodium dodecyl sulfate-polyacrylamide gel electrophoresis (SDS-PAGE) and, subsequently, western blot was carried out. IGFBP-3 was determined by using a biotinylated anti-hIGFBP-3 antibody. Exposure time was 2 s (**a**). Membrane, matrix and the two core fractions of sucrose purified P13-SigE7Lamp-TK$^-$, P13-SigE7Lamp-H5-IGFBP-3 and P13-SigE7Lamp-H5-IGFBP-3(b) were prepared to determine whether IGFBP-3 integrates into specific parts of the virion. Each fraction was separated by 10% SDS-PAGE and subjected to subsequent western blot (**b**). To determine whether IGFBP-3 influences the protein composition of the VACV, sucrose purified virions of P13-SigE7Lamp-TK$^-$, P13-SigE7Lamp-H5-IGFBP-3 and P13-SigE7Lamp-E/L-IGFBP-3 viruses were separated by 10% SDS-PAGE and the gel was stained with Coomassie brilliant blue (**c**).

plaques per Petri dish. Then, rabbit VACV neutralizing serum or nonimmune serum was added for 1 h. Finally, the cells were overlaid with agar with the medium and the plaques formed were counted after 3 days (Figure 7). We observed no differences between infected cells cultured in the medium or in the medium containing nonimmune serum. In the presence of VACV-neutralizing serum, P13-SigE7Lamp-H5-IGFBP-3 formed significantly (**$P<0.01$) more plaques than P13-SigE7Lamp-TK$^-$. This shows that the rate of virus entry into CV1 cells was higher for P13-SigE7Lamp-H5-IGFBP-3 than for P13-SigE7Lamp-TK$^-$.

Finally, to rule out the possibility that the difference in virus entry is caused by enhanced virus adsorption, we determined the amount of unadsorbed virus in the supernatant. CV-1 cells were infected with P13-SigE7Lamp-TK$^-$ or P13-SigE7Lamp-H5-IGFBP-3 as in the previous experiment. The inoculum from four parallels was removed, mixed and frozen at indicated intervals and virus

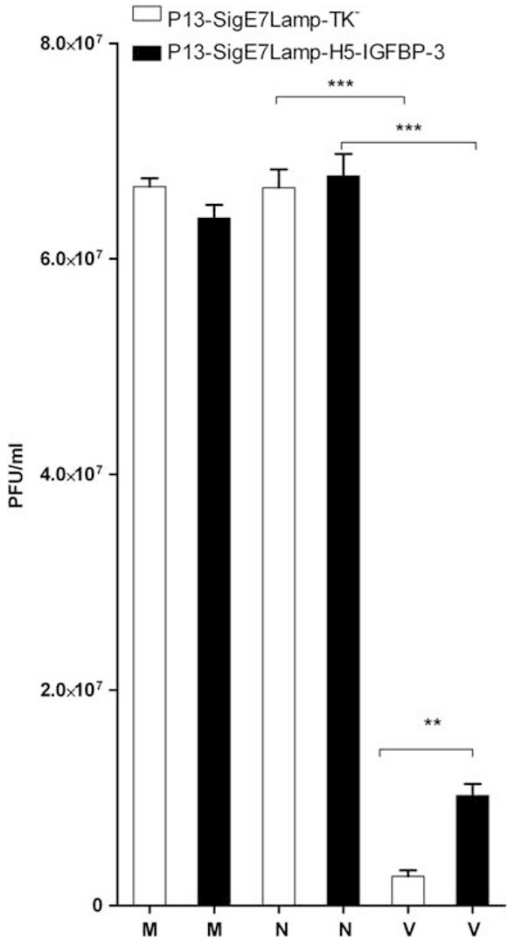

Figure 7. Insulin-like growth factor-binding protein-3 (IGFBP-3) enhances recombinant vaccinia virus (rVACV) cell penetration. CV-1 cells were inoculated with equally prepared virus suspensions of P13-SigE7Lamp-TK$^-$ and P13-SigE7Lamp-H5-IGFBP-3 diluted 10^{-5}. After 1.5 h of adsorption, the medium (M), nonimmune rabbit serum (N) or neutralizing anti-VACV rabbit serum (V) was added for 1 h. The inoculum was removed and cell cultures were overlaid with 1% agar supplemented with Eagle's minimum essential medium (E-MEM) with 5% fetal bovine serum (FBS). After 3 days at 37 °C, agar supplemented with the medium and neutral red was overlaid and the plaque-forming unit (PFU) count was determined. Each value represents the arithmetic mean of five parallels. Results were analyzed and statistics were calculated using one-way analysis of variance (ANOVA). $^{**}P<0.01$, $^{***}P<0.001$.

titer was determined in quintuplicates (Figure 8). We found out that the adsorption rate is similar for P13-SigE7Lamp-TK$^-$ and P13-SigE7Lamp- H5-IGFBP-3 at adsorption times up to 1 h; however, the depletion of P13-SigE7Lamp-H5-IGFBP-3 from the inoculum was significantly ($^*P=0.0205$) higher than that of P13-SigE7Lamp-TK$^-$ at adsorption time of 1.5 h and also higher at 2 h, although not significantly. The experiment was repeated twice with similar results.

Taken together, the higher adsorption rate contributed to better virus entry of P13-SigE7Lamp-H5-IGFBP-3 and better overall replication when compared with P13-SigE7Lamp-TK$^-$.

The surface of P13-SigE7Lamp-H5-IGFBP-3 virions has higher PS content than P13-SigE7Lamp-TK$^-$

To further define structural differences that could underlie higher adsorption rate of *P13-SigE7Lamp-H5-IGFBP-3* virus, we developed

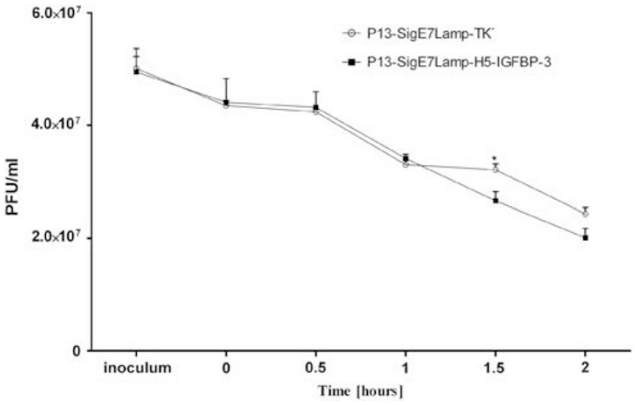

Figure 8. Insulin-like growth factor-binding protein-3 (IGFBP-3) enhances adsorption of recombinant vaccinia virus (rVACV) on CV-1 cells. Virus adsorption was determined as the amount of unadsorbed plaque-forming units (PFUs). Equal suspensions of P13-SigE7Lamp-TK$^-$ and P13-SigE7Lamp-H5-IGFBP-3 that contain the same amount of viruses were prepared. These suspensions were added to confluently grown CV-1 cells. At each interval, the inoculum was removed and titrated to determine the amount of PFUs. Each value represents the arithmetic mean of five parallels. Results were analyzed and statistics were calculated using Student's *t*-test. $^*P<0.05$.

an assay for detection of the PS present on the surface of purified IMVs. For this purpose, a fluorescence detection system using virions immobilized on microbeads through anti-virus antibody as described originally for HIV-1-like particles[59] has been adapted. The specificity of the assay has been proven in following steps. The G-protein-coated beads were covered with VACV virions as described in the Materials and methods. First, the binding of mouse IgG to G protein on beads was demonstrated by staining with the secondary antibody (Supplementary Figure 1). Subsequently, specific binding of IMVs to beads was confirmed by staining with rabbit anti-VACV serum and secondary anti-rabbit conjugate. The mean fluorescent intensity of beads was highest if beads were covered with a sandwich of VACV-positive mouse serum, VACV virions and anti-VACV rabbit antibodies. A weaker signal was obtained if nonimmune mouse serum was used (Supplementary Figure 2). To determine PS content in a sample of IMVs, the beads carrying purified P13-SigE7Lamp-H5-IGFBP-3 or P13-SigE7Lamp TK$^-$ IMVs or beads without virions (PBS) were stained with annexin V. Beads covered with P13-SigE7Lamp-H5-IGFBP-3 had higher mean fluorescence intensity than beads covered with P13-SigE7LampTK$^-$ (Figure 9). The fluorescence was lower if no virions or nonimmune mouse serum has been added to beads. To confirm elevation of PS in viruses that produce high amount of IGFBP3, the experiment was repeated with lower amount of virions (20 μg) and also with independently derived viruses. P13-SigE7Lamp-H5-IGFBP-3 and P13-SigE7Lamp-H5-IGFBP-3(b), P13-SigE7Lamp-TK$^-$ and P13-SigE7Lamp-TK$^-$(b) bound to beads were stained with annexin V. The difference was the similar for both sister viruses (Supplementary Figure 3).

DISCUSSION

In the present study, we are the first to describe recombinant vaccinia viruses expressing the tumor suppressor gene *IGFBP-3*. These viruses have been engineered to coexpress IGFBP-3 with the immunogenic fusion protein SigE7Lamp. Our original hypothesis was that high-level expression of IGFBP-3 by rVACV could inhibit the growth of tumors in our HPV16 E7-induced cervical cancer model, which would give time to the anti-E7 immune response to develop. We expected that tumors treated with

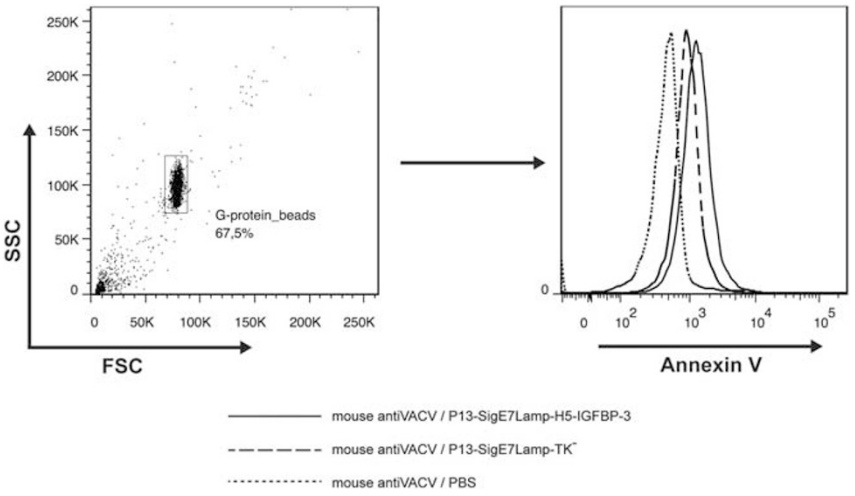

Figure 9. Phosphatidylserine content is elevated in virions of P13-SigE7Lamp-H5-IGFBP-3. Equal amount of virions of P13-SigE7Lamp-H5-IGFBP-3, P13-SigE7Lamp-TK$^-$ or phosphate-buffered saline (PBS) were added to G-protein beads coated with mouse antiVACV serum and incubated for 3 h. In the next step, the beads were incubated with blocking buffer, washed and phycoerythrin (PE)-labeled annexin V was added for 15 min. Fluorescence intensity was measured using flow cytometry. The gating strategy for microbeads is shown. FSC, forward scatter; IGFBP-3, insulin-like growth factor-binding protein-3; SSC, side scatter.

IGFBP-3-expressing viruses would grow at slow rate and would be more readily controlled by the mounted immune response.

In the initial phase after virus construction, we had to characterize the IGFBP-3- expressing VACV viruses as no information was available in the literature. We have found several differences between the viruses P13-SigE7Lamp-H5-IGFBP-3, P13-SigE7Lamp-E/L-IGFBP-3 and the control virus P13-SigE7Lamp-TK$^-$. First, P13-SigE7Lamp-H5-IGFBP-3 produced higher amounts of IGFBP-3 than P13-SigE7Lamp-E/L-IGFBP-3. The expression under the control of the synthetic E/L promoter is usually very strong as we have observed for expression of interleukin-12,[60] or soluble form of Flt3L.[11] On the other hand, we have already prepared several rVACVs where a too high expression of a protein was incompatible with the formation of an infectious virus and where the expression under the H5 promoter gave higher yields of the transgenic product, as was the case of the P13-TβRII viruses.[61] Toxicity of high levels of IGFBP-3 (under sE/L promoter) can be connected with induction of apoptosis that, in vaccination strain Praha, is not fully inhibited by antiapoptotic mechanisms as in other VACV strains (for example, WR strain).[62] Second, the analysis of immunogenicity revealed that both P13-SigE7Lamp-H5-IGFBP-3 and P13-SigE7Lamp-E/L-IGFBP-3 elicited higher anti-VACV responses than P13-SigE7Lamp-TK$^-$, although not statistically significantly because of the high variability.

The next step was to test the therapeutic potential of P13-SigE7Lamp-H5-IGFBP-3 and P13-SigE7Lamp-E/L-IGFBP-3 in our *in vivo* cancer model. Again, we observed noteworthy differences between the viruses. Mice treated with SigE7Lamp-H5-IGFBP-3 had significantly smaller tumors than PBS-treated mice since day 11, whereas in the mice treated with P13-SigE7Lamp-E/L-IGFBP-3 and P13-SigE7Lamp-TK$^-$, significantly smaller tumors were first found on day 18. Furthermore, by day 32, the tumors of mice immunized with P13-SigE7Lamp-H5-IGFBP-3 were smaller than after treatment with P13-SigE7Lamp-TK$^-$, whereas the tumors of mice treated with P13-SigE7Lamp-E/L-IGFBP-3 showed no significant difference when compared with P13-SigE7Lamp-TK$^-$. The higher efficacy of P13- SigE7Lamp-H5-IGFBP-3 was expected, in agreement with the observed higher production of IGFBP-3.

Next, we wanted to characterize the replication of IGFBP-3-expressing rVACVs and to learn whether these viruses replicate better than the control. Results from quantitative PCR indicate that P13-SigE7Lamp-H5-IGFBP-3 virus replication was higher in comparison with the other viruses. To analyze this observation, we decided to test the virus *in vitro* on CV-1 and TC-1 cell cultures. These two cell lines were selected to test virus replication because CV-1 is a standard cell line for virus titration and TC-1 cells are used in the murine tumor model. The *in vitro* tests confirmed that P13-SigE7Lamp-H5-IGFBP-3 replication is higher when compared with the other viruses regardless of the cell line used. P13-SigE7Lamp-E/L-IGFBP-3 exhibited higher replication than P13-SigE7Lamp-TK$^-$ but only when CV-1 cells were used. We assumed that high-level IGFBP-3 expression by P13-SigE7Lamp-H5-IGFBP-3 influenced viral replication. We decided to use the polyclonal neutralizing anti-IGFBP-3 antibody AF675 (anti-human IGFBP-3, R&D Systems) to determine the role of IGFBP-3. Indeed, our results showed that even partial IGFBP-3 neutralization was sufficient to decrease virus yields. In contrast, the same antibody increased the yields of P13-SigE7Lamp-TK$^-$. This can be attributed to the fact that IGFBP-3 accumulated in aged CV-1 cell cultures and was probably used to downregulate their metabolic activity. Complete IGFBP-3 neutralization could inhibit this decrease in metabolic activity. More metabolically active cells support better virus replication. We have shown previously that high expression of Flt3 ligand by rVACV led to its incorporation into IMV and to structural changes in virions causing virus attenuation *in vivo*.[58] The incorporation of the foreign gene product in the poxvirus virion has been reported previously for a number of recombinant proteins.[57,63–65] The proteins can be trapped into one or more virion compartments. We therefore decided to analyze sucrose gradient purified IMV of P13-SigE7Lamp-H5-IGFBP-3, P13-SigE7Lamp-E/L-IGFBP-3, P13-SigE7Lamp-TK$^-$ and their respective independently prepared sister viruses. Comparison of the sister viruses was necessary to exclude the influence of casual mutations. Western blot analysis revealed at least four bands in the IMVs of P13-SigE7Lamp-H5-IGFBP-3 (Figure 6). A weak signal was also detected in the IMVs of P13-SigE7Lamp-E/L-IGFBP-3, indicating a lower amount of the integrated protein. No signal was detected in the IMVs of the control virus. The band I that corresponds to glycosylated IGFBP-3 was detected in all virion fractions except the membranous envelope.

We speculate that the observed smaller bands II and III represent either nonglycosylated IGFBP-3 and/or products of proteolytic cleavage of IGFBP-3 by VACV proteases during virus maturation. This speculation is based on the fact that

VACV-encoded proteases recognize protein sequences AGX (where X can be A, S or T but not N)[66] that can be found in IGFBP-3. The larger band could represent a complex containing IGFBP-3. In the next step, we analyzed whether IGFBP-3 incorporation changed the protein content of IMV. Coomassie blue staining of SDS-PAGE-separated IMVs did not show any differences between the IGFBP-3-expressing viruses and P13-SigE7Lamp-TK$^-$.

Finally, we analyzed which phase of the viral replication cycle is influenced by IGFBP-3, and found that cell adsorption of P13-SigE7Lamp-H5-IGFBP-3 is enhanced when compared with P13-SigE7Lamp-TK$^-$. We supposed that IGFBP-3 integration or other structural difference could help the early stages of virus replication—that is, virus adsorption and/or virus entry. The initial steps of virus replication were analyzed in two independent experiments with the same outcome: the IGFBP-3 producing recombinant is adsorbed at a higher rate. The higher virus adsorption was demonstrated in an experiment where infection has been stopped by virus neutralization with VACV-specific antibodies (Figure 7) and in another experiment where the amount of nonadsorbed virus was determined (Figure 8) and where the result was not dependent on the use of antibodies.

In the present report an explanation of higher adsorption rate of IGFBP-3-expressing virus is suggested. We experimentally uncovered structural difference between the IMVs of VACV expressing high-level IGFBP-3 and a control virus that consists of distinct PS exposure on IMV membrane. We suppose that formation of IMV in cells containing large concentration of the apoptosis inducer IGFBP-3 could result in assembly of IMVs with elevated PS content that are macropinocytosed at higher rate. The result is important because it suggests that modification of PS content in IMV is feasible and can result in changes in virus multiplication. Besides, we introduced a new assay for analyzing composition of VACV IMVs. However it cannot be ruled out that direct interactions of IGFBP-3 incorporated in IMV with cellular protein can contribute to increased virus adsorption, as the experiments with IGFBP-3-neutralizing antibody suggested. It has been shown that the C-terminal part of IGFBP-3 contains domains that bind different components of the extracellular matrix and caveolin-1.[28] In addition, peptides derived from the heparin-binding domain of IGFBP-3 can be used as protein carriers for protein cell delivery.[67] Furthermore, early stages of IGFBP-3 cellular uptake are in part mediated through macropinocytosis, which is also a major route for VACV entry.[32]

However, it is to be assumed that, in this case, incorporation of IGFBP-3 to viron membrane would be required. But structural analysis revealed only trace amounts of IGFBP-3 in the membrane fraction of IMV.

CONCLUSION

Based on the presented results, we propose a model in which high-level expression of IGFBP-3 by P13-SigE7Lamp-H5-IGFBP-3 leads to its incorporation into the progeny IMVs and to elevated PS content. These IMVs can then infect cells more efficiently that results in longer persistence of the rVACV and longer immune stimulation that in turn slows down the growth of TC-1 tumors.

CONFLICT OF INTEREST

The authors declare no conflict of interest.

ACKNOWLEDGEMENTS

We thank W Zwerschke (Universität Innsbruck) for kindly providing the pXBP-3-WT plasmid and TC Wu (Johns Hopkins Medical Institutions, Baltimore) for providing the TC-1 cell line. This work was supported by project for the conceptual development of research organization, VZ MZ 00002373601 IHBT of the Ministry of Health of the Czech Republic and ERDF OPPK CZ.2.16/3.1.00/24001.

REFERENCES

1 Mackett M, Smith GL. Vaccinia virus expression vectors. *J Gen Virol* 1986; **67**: 2067–2082.
2 Chakrabarti S, Sisler JR, Moss B. Compact, synthetic, vaccinia virus early/late promoter for protein expression. *Biotechniques* 1997; **23**: 1094–1097.
3 Kantor J, Irvine K, Abrams S, Kaufman H, DiPietro J, Schlom J. Antitumor activity and immune responses induced by a recombinant carcinoembryonic antigen-vaccinia virus vaccine. *J Natl Cancer Inst* 1992; **84**: 1084–1091.
4 Hodge JW, Schlom J, Donohue SJ, Tomaszewski JE, Wheeler CW, Levine BS *et al.* A recombinant vaccinia virus expressing human prostate-specific antigen (PSA): safety and immunogenicity in a non-human primate. *Int J Cancer* 1995; **63**: 231–237.
5 Balloul JM, Acres RB, Geist M, Dott K, Stefani L, Schmitt D *et al.* Recombinant MUC 1 vaccinia virus: a potential vector for immunotherapy of breast cancer. *Cell Mol Biol (Noisy-le-grand)* 1994; **40**(Suppl 1): 49–59.
6 Mulryan K, Ryan MG, Myers KA, Shaw D, Wang W, Kingsman SM *et al.* Attenuated recombinant vaccinia virus expressing oncofetal antigen (tumor-associated antigen) 5T4 induces active therapy of established tumors. *Mol Cancer Ther* 2002; **1**: 1129–1137.
7 Smith CL, Dunbar PR, Mirza F, Palmowski MJ, Shepherd D, Gilbert SC *et al.* Recombinant modified vaccinia Ankara primes functionally activated CTL specific for a melanoma tumor antigen epitope in melanoma patients with a high risk of disease recurrence. *Int J Cancer* 2005; **113**: 259–266.
8 Aarts WM, Schlom J, Hodge JW. Vector-based vaccine/cytokine combination therapy to enhance induction of immune responses to a self-antigen and anti-tumor activity. *Cancer Res* 2002; **62**: 5770–5777.
9 Rochlitz C, Figlin R, Squiban P, Salzberg M, Pless M, Herrmann R *et al.* Phase I immunotherapy with a modified vaccinia virus (MVA) expressing human MUC1 as antigen-specific immunotherapy in patients with MUC1-positive advanced cancer. *J Gene Med* 2003; **5**: 690–699.
10 Yang AS, Monken CE, Lattime EC. Intratumoral vaccination with vaccinia-expressed tumor antigen and granulocyte macrophage colony-stimulating factor overcomes immunological ignorance to tumor antigen. *Cancer Res* 2003; **63**: 6956–6961.
11 Zurkova K, Babiarova K, Hainz P, Krystofova J, Kutinova L, Otahal P *et al.* The expression of the soluble isoform of hFlt3 ligand by recombinant vaccinia virus enhances immunogenicity of the vector. *Oncol Rep* 2009; **21**: 1335–1343.
12 Jager E, Karbach J, Gnjatic S, Neumann A, Bender A, Valmori D *et al.* Recombinant vaccinia/fowlpox NY-ESO-1 vaccines induce both humoral and cellular NY-ESO-1-specific immune responses in cancer patients. *Proc Natl Acad Sci USA* 2006; **103**: 14453–14458.
13 Madan RA, Arlen PM, Mohebtash M, Hodge JW, Gulley JL. Prostvac-VF: a vector-based vaccine targeting PSA in prostate cancer. *Expert Opin Investig Drugs* 2009; **18**: 1001–1011.
14 Kim DW, Krishnamurthy V, Bines SD, Kaufman HL. TroVax, a recombinant modified vaccinia Ankara virus encoding 5T4: lessons learned and future development. *Hum Vaccin* 2010; **6**: 784–791.
15 Oudard S, Rixe O, Beuselinck B, Linassier C, Banu E, Machiels JP *et al.* A phase II study of the cancer vaccine TG4010 alone and in combination with cytokines in patients with metastatic renal clear-cell carcinoma: clinical and immunological findings. *Cancer Immunol Immunother* 2011; **60**: 261–271.
16 Smith CL, Mirza F, Pasquetto V, Tscharke DC, Palmowski MJ, Dunbar PR *et al.* Immunodominance of poxviral-specific CTL in a human trial of recombinant-modified vaccinia Ankara. *J Immunol* 2005; **175**: 8431–8437.
17 Smith GL. Vaccinia virus immune evasion. *Immunol Lett* 1999; **65**: 55–62.
18 Perdiguero B, Esteban M. The interferon system and vaccinia virus evasion mechanisms. *J Interferon Cytokine Res* 2009; **29**: 581–598.
19 Mercer J, Helenius A. Vaccinia virus uses macropinocytosis and apoptotic mimicry to enter host cells. *Science* 2008; **320**: 531–535.
20 Zapf J, Schoenle E, Jagars G, Sand I, Grunwald J, Froesch ER. Inhibition of the action of nonsuppressible insulin-like activity on isolated rat fat cells by binding to its carrier protein. *J Clin Invest* 1979; **63**: 1077–1084.
21 Spagnoli A, Torello M, Nagalla SR, Horton WA, Pattee P, Hwa V *et al.* Identification of STAT-1 as a molecular target of IGFBP-3 in the process of chondrogenesis. *J Biol Chem* 2002; **277**: 18860–18867.
22 Kielczewski JL, Jarajapu YP, McFarland EL, Cai J, Afzal A, Li CS *et al.* Insulin-like growth factor binding protein-3 mediates vascular repair by enhancing nitric oxide generation. *Circ Res* 2009; **105**: 897–905.
23 Yoon IK, Kim HK, Kim YK, Song IH, Kim W, Kim S *et al.* Exploration of replicative senescence-associated genes in human dermal fibroblasts by cDNA microarray technology. *Exp Gerontol* 2004; **39**: 1369–1378.
24 Elzi DJ, Lai Y, Song M, Hakala K, Weintraub ST, Shiio Y. Plasminogen activator inhibitor 1--insulin-like growth factor binding protein 3 cascade regulates stress-induced senescence. *Proc Natl Acad Sci USA* 2012; **109**: 12052–12057.
25 Clemmons DR. Insulin-like growth factor binding proteins and their role in controlling IGF actions. *Cytokine Growth Factor Rev* 1997; **8**: 45–62.

26 Meinbach DS, Lokeshwar BL. Insulin-like growth factors and their binding proteins in prostate cancer: cause or consequence? *Urol Oncol* 2006; **24**: 294–306.
27 Alami N, Page V, Yu Q, Jerome L, Paterson J, Shiry L *et al.* Recombinant human insulin-like growth factor-binding protein 3 inhibits tumor growth and targets the Akt pathway in lung and colon cancer models. *Growth Horm IGF Res* 2008; **18**: 487–496.
28 Yamada PM, Lee KW. Perspectives in mammalian IGFBP-3 biology: local vs. systemic action. *Am J Physiol Cell Physiol* 2009; **296**: C954–C976.
29 Ingermann AR, Yang YF, Han J, Mikami A, Garza AE, Mohanraj L *et al.* Identification of a novel cell death receptor mediating IGFBP-3-induced anti-tumor effects in breast and prostate cancer. *J Biol Chem* 2010; **285**: 30233–30246.
30 Lee YC, Jogie-Brahim S, Lee DY, Han J, Harada A, Murphy LJ *et al.* Insulin-like growth factor-binding protein-3 (IGFBP-3) blocks the effects of asthma by negatively regulating NF-kappaB signaling through IGFBP-3R-mediated activation of caspases. *J Biol Chem* 2011; **286**: 17898–17909.
31 Han J, Jogie-Brahim S, Harada A, Oh Y. Insulin-like growth factor-binding protein-3 suppresses tumor growth via activation of caspase-dependent apoptosis and cross-talk with NF-kappaB signaling. *Cancer Lett* 2011; **307**: 200–210.
32 Micutkova L, Hermann M, Offterdinger M, Hess MW, Matscheski A, Pircher H *et al.* Analysis of the cellular uptake and nuclear delivery of insulin-like growth factor binding protein-3 in human osteosarcoma cells. *Int J Cancer* 2012; **130**: 1544–1557.
33 Lee KW, Liu B, Ma L, Li H, Bang P, Koeffler HP *et al.* Cellular internalization of insulin-like growth factor binding protein-3: distinct endocytic pathways facilitate re-uptake and nuclear localization. *J Biol Chem* 2004; **279**: 469–476.
34 Singh B, Charkowicz D, Mascarenhas D. Insulin-like growth factor-independent effects mediated by a C-terminal metal-binding domain of insulin-like growth factor binding protein-3. *J Biol Chem* 2004; **279**: 477–487.
35 Schedlich LJ, Le Page SL, Firth SM, Briggs LJ, Jans DA, Baxter RC. Nuclear import of insulin-like growth factor-binding protein-3 and -5 is mediated by the importin beta subunit. *J Biol Chem* 2000; **275**: 23462–23470.
36 Lee KW, Ma L, Yan X, Liu B, Zhang XK, Cohen P. Rapid apoptosis induction by IGFBP-3 involves an insulin-like growth factor-independent nucleomitochondrial translocation of RXRalpha/Nur77. *J Biol Chem* 2005; **280**: 16942–16948.
37 Kim HS, Lee WJ, Lee SW, Chae HW, Kim DH, Oh Y. Insulin-like growth factor binding protein-3 induces G1 cell cycle arrest with inhibition of cyclin-dependent kinase 2 and 4 in MCF-7 human breast cancer cells. *Horm Metab Res* 2010; **42**: 165–172.
38 Wu C, Liu X, Wang Y, Tian H, Xie Y, Li Q *et al.* Insulin-like factor binding protein-3 promotes the G1 cell cycle arrest in several cancer cell lines. *Gene* 2012; **512**: 127–133.
39 Martin JL, Baxter RC. Oncogenic ras causes resistance to the growth inhibitor insulin-like growth factor binding protein-3 (IGFBP-3) in breast cancer cells. *J Biol Chem* 1999; **274**: 16407–16411.
40 Hanafusa T, Yumoto Y, Nouso K, Nakatsukasa H, Onishi T, Fujikawa T *et al.* Reduced expression of insulin-like growth factor binding protein-3 and its promoter hypermethylation in human hepatocellular carcinoma. *Cancer Lett* 2002; **176**: 149–158.
41 Ibanez dC I, Dulaimi E, Hoffman AM, Al-Saleem T, Uzzo RG, Cairns P. Identification of novel target genes by an epigenetic reactivation screen of renal cancer. *Cancer Res* 2006; **66**: 5021–5028.
42 Tomii K, Tsukuda K, Toyooka S, Dote H, Hanafusa T, Asano H *et al.* Aberrant promoter methylation of insulin-like growth factor binding protein-3 gene in human cancers. *Int J Cancer* 2007; **120**: 566–573.
43 Lu XF, Jiang XG, Lu YB, Bai JH, Mao ZB. Characterization of a novel positive transcription regulatory element that differentially regulates the insulin-like growth factor binding protein-3 (IGFBP-3) gene in senescent cells. *J Biol Chem* 2005; **280**: 22606–22615.
44 Bowen C, Bubendorf L, Voeller HJ, Slack R, Willi N, Sauter G *et al.* Loss of NKX3.1 expression in human prostate cancers correlates with tumor progression. *Cancer Res* 2000; **60**: 6111–6115.
45 Muhlbradt E, Asatiani E, Ortner E, Wang A, Gelmann EP. NKX3.1 activates expression of insulin-like growth factor binding protein-3 to mediate insulin-like growth factor-I signaling and cell proliferation. *Cancer Res* 2009; **69**: 2615–2622.
46 Santer FR, Bacher N, Moser B, Morandell D, Ressler S, Firth SM *et al.* Nuclear insulin-like growth factor binding protein-3 induces apoptosis and is targeted to ubiquitin/proteasome-dependent proteolysis. *Cancer Res* 2006; **66**: 3024–3033.
47 Santer FR, Moser B, Spoden GA, Jansen-Durr P, Zwerschke W. Human papillomavirus type 16 E7 oncoprotein inhibits apoptosis mediated by nuclear insulin-like growth factor-binding protein-3 by enhancing its ubiquitin/proteasome-dependent degradation. *Carcinogenesis* 2007; **28**: 2511–2520.
48 Nemeckova S, Stranska R, Subrtova J, Kutinova L, Otahal P, Hainz P *et al.* Immune response to E7 protein of human papillomavirus type 16 anchored on the cell surface. *Cancer Immunol Immunother* 2002; **51**: 111–119.
49 Kutinova L, Ludvikova V, Simonova V, Otavova M, Krystofova J, Hainz P *et al.* Search for optimal parent for recombinant vaccinia virus vaccines. Study of three vaccinia virus vaccinal strains and several virus lines derived from them. *Vaccine* 1995; **13**: 487–493.
50 Mackova J, Kutinova L, Hainz P, Krystofova J, Sroller V, Otahal P *et al.* Adjuvant effect of dendritic cells transduced with recombinant vaccinia virus expressing HPV16-E7 is inhibited by co-expression of IL12. *Int J Oncol* 2004; **24**: 1581–1588.
51 Perkus ME, Panicali D, Mercer S, Paoletti E. Insertion and deletion mutants of vaccinia virus. *Virology* 1986; **152**: 285–297.
52 Kutinova L, Nemeckova S, Hamsikova E, Zavadova H, Ludvikova V, Broucek J *et al.* Hepatitis B virus proteins expressed by recombinant vaccinia viruses: influence of preS2 sequence on expression surface and nucleocapsid proteins in human diploid cells. *Arch Virol* 1994; **134**: 1–15.
53 Joklik WK. The purification fo four strains of poxvirus. *Virology* 1962; **18**: 9–18.
54 Lin KY, Guarnieri FG, Staveley-O'Carroll KF, Levitsky HI, August JT, Pardoll DM *et al.* Treatment of established tumors with a novel vaccine that enhances major histocompatibility class II presentation of tumor antigen. *Cancer Res* 1996; **56**: 21–26.
55 Smahel M, Sobotkova E, Bubenik J, Simova J, Zak R, Ludvikova V *et al.* Metastatic MHC class I-negative mouse cells derived by transformation with human papillomavirus type 16. *Br J Cancer* 2001; **84**: 374–380.
56 Gabriel P, Babiarova K, Zurkova K, Krystofova J, Hainz P, Kutinova L *et al.* Chemokine binding protein vCCI attenuates vaccinia virus without affecting the cellular response elicited by immunization with a recombinant vaccinia vector carrying the HPV16 E7 gene. *Viral Immunol* 2012; **25**: 411–422.
57 Gomez CE, Esteban M. Recombinant proteins produced by vaccinia virus vectors can be incorporated within the virion (IMV form) into different compartments. *Arch Virol* 2001; **146**: 875–892.
58 Zurkova K, Hainz P, Krystofova J, Kutinova L, Sanda M, Nemeckova S. Attenuation of vaccinia virus by the expression of human Flt3 ligand. *Virol J* 2010; **7**: 109.
59 Kim BC, Ju MK, Dan-Chin-Yu A, Sommer P. Quantitative detection of HIV-1 particles using HIV-1 neutralizing antibody-conjugated beads. *Anal Chem* 2009; **81**: 2388–2393.
60 Nemeckova S, Sroller V, Hainz P, Krystofova J, Smahel M, Kutinova L. Experimental therapy of HPV16 induced tumors with IL12 expressed by recombinant vaccinia virus in mice. *Int J Mol Med* 2003; **12**: 789–796.
61 Zurkova K, Chlanda P, Samkova Z, Babiarova K, Kutinova L, Krystofova J *et al.* Expression of soluble TGF-beta receptor II by recombinant Vaccinia virus enhances E7 specific immunotherapy of HPV16 tumors. *Neoplasma* 2011; **58**: 181–188.
62 Liskova J, Knitlova J, Honner R, Melkova Z. Apoptosis and necrosis in vaccinia virus-infected HeLa G and BSC-40 cells. *Virus Res* 2011; **160**: 40–50.
63 Morrison DK, Moyer RW. Detection of a subunit of cellular Pol II within highly purified preparations of RNA polymerase isolated from rabbit poxvirus virions. *Cell* 1986; **44**: 587–596.
64 Franke CA, Hruby DE. Association of non-viral proteins with recombinant vaccinia virus virions. *Arch Virol* 1987; **94**: 347–351.
65 Bereta M, Bereta J, Park J, Medina F, Kwak H, Kaufman HL. Immune properties of recombinant vaccinia virus encoding CD154 (CD40L) are determined by expression of virally encoded CD40L and the presence of CD40L protein in viral particles. *Cancer Gene Ther* 2004; **11**: 808–818.
66 Byrd CM, Hruby DE. Vaccinia virus proteolysis--a review. *Rev Med Virol* 2006; **16**: 187–202.
67 Goda N, Tenno T, Inomata K, Shirakawa M, Tanaka T, Hiroaki H. Intracellular protein delivery activity of peptides derived from insulin-like growth factor binding proteins 3 and 5. *Exp Cell Res* 2008; **314**: 2352–2361.

Supplementary Information accompanies the paper on Cancer Gene Therapy website (http://www.nature.com/cgt)